Open Access Full Text Article

ORIGINAL RESEARCH

A Modified Targetoid Feature Emphasizing Thin-Rim APHE to Improve the Diagnostic Performance of LI-RADS for Malignant Hepatic Tumors

Runqian Huang[1],*, Chunling Zheng [1,2],*, Guixiao Xu[1], Xuanwei Chen[1], Jingxian Shen [1], Siyue Mao[1]

[1]Department of Radiology, State Key Laboratory of Oncology in South China, Guangdong Provincial Clinical Research Center for Cancer, Sun Yat-Sen University Cancer Center, Guangzhou, 510060, People's Republic of China; [2]Department of Radiology, The Sixth Affiliated Hospital, Sun Yat-Sen University, Guangzhou, Guangdong Province, People's Republic of China

*These authors contributed equally to this work

Correspondence: Jingxian Shen; Siyue Mao, Department of Radiology, State Key Laboratory of Oncology in South China, Guangdong Provincial Clinical Research Center for Cancer, Sun Yat-sen University Cancer Center, Sun Yat-sen University, 651 Dongfeng Road East, Guangzhou, 510060, People's Republic of China, Tel/Fax +86-20-87343217, Email shenjx@sysucc.org.cn; maosiy@sysucc.org.cn

Objective: To identify imaging features that help distinguish between HCCs and non-HCC malignancies assigned to LI-RADS M (LR-M) and evaluate the diagnostic performance of a LI-RADS with targetoid criteria using thin-rim arterial phase hyperenhancement (APHE).

Materials and Methods: This retrospective study included 381 patients (387 observations) at high-risk for HCC who underwent enhanced-MRI before surgery. Three radiologists reviewed images for LI-RADS categorization of hepatic observations. Univariate and multivariate analysis was conducted to determine reliable features to differentiate between HCC and non-HCC malignancies among the LR-M lesions. The thin-rim (<30%) APHE was defined based on the thickest thickness of rim APHE compared with the tumor radius, and a modified LI-RADS emphasizing thin-rim APHE as a specific feature of LR-M was established. We compared the diagnostic performance of modified LR-M and LI-RADS 5 (LR-5) with the conventional one.

Results: Thin-rim APHE and targetoid diffusion-weighted imaging (DWI) were found as independent predictive factors of non-HCC malignancies, while enhancing capsule, thick-rim APHE and peripheral washout were noted as independent variables significantly associated with HCC of LR-M ($P<0.05$). The noticeable diagnostic performance of thin-rim APHE in distinguishing non-HCC malignancies from HCCs using the ROC curve. Emphasizing thin-rim APHE on targetoid features, the modified LR-M revealed significantly superior specificity and accuracy (89.4% vs 81.1%, $P=0.004$; and 87.9% vs 82.2%, $P=0.027$, respectively) while maintaining high sensitivity (82.2% vs 86.0%; $P=0.529$) compared with the LR-M. Meanwhile, the modified LR-5 achieved greater sensitivity and accuracy (88.6% vs 79.7%, $P=0.004$; and 85.8% vs 80.1%, $P=0.036$, respectively) for diagnosing HCC, without compromising specificity (78.3% vs.81.1%; $P=0.608$) compared with the LR-5.

Conclusion: Thin-rim APHE may be the specific imaging feature for differentiating non-HCC malignancies from HCCs within LR-M. The modified targetoid criteria emphasizing thin-rim APHE can improve the diagnostic performance of LI-RADS for hepatic malignancies.

Keywords: hepatic tumors, malignant, targetoid feature, Rim APHE, liver imaging reporting and data system

Introduction

The Liver Imaging Reporting and Data System version 2018 (LI-RADS v2018) aims to standardize the interpretation and reporting of hepatic lesions in patients who are at a high-risk of hepatocellular carcinoma (HCC).[1–3] In these patients, the distinction between HCCs and non-HCC malignancies is important for improving therapeutic and prognostic methods.[4–7]

775

Therefore, the LI-RADS v2018 provides a LI-RADS M (LR-M) category for hepatic observations that may reflect malignancy, while it is unspecific to HCC.[1] Hepatic observations showing any targetoid features, such as rim arterial-phase hyperenhancement (APHE), peripheral washout, delayed central enhancement and targetoid appearance on diffusion-weighted imaging (DWI) or transitional phase/hepatobiliary phase (TP/HBP), can be categorized into LR-M category.[1] A meta-analysis[8] that involved 1819 LR-M lesions from 10 studies demonstrated that among the LR-M imaging features, rim APHE showed the highest pooled frequency in both non-HCC malignancies (48.9%) and HCCs (9.8%). Besides, as reported by Kim et al,[9] rim APHE was the most sensitive feature of LR-M, and it was highly valuable for classifying non-HCC malignancies in patients with liver cirrhosis.

Though the LR-M imaging features was commonly used to characterize non-HCC malignancies, which mostly presented as intrahepatic cholangiocarcinoma (ICC) and combined hepatocellular-cholangiocarcinoma (cHCC-CC),[10–14] previous studies have shown that the LR-M category had a relatively low specificity (48–54%)[9,15] for non-HCC malignancies and 28–36% of atypical HCCs might be classified as LR-M [3; 9; 10], as these HCCs could also have targetoid features [8; 11–13]. Therefore, it is important to identify non-HCC malignancies from HCCs and to improve the accuracy of the LR-M category. A number of scholars studied on MRI features for distinguishing HCC with targetoid features from non-HCC malignancy within LR-M, and valuable imaging features, such as enhancing capsule and some ancillary imaging features, were found.[13,16–18] However, enhancing capsule was more commonly associated with extracellular agent MRI (ECA-MRI) compared with hepatobiliary agent MRI (HBA-MRI), because of the peculiar characteristics of gadoxetic acid that could cause enhancement of the liver parenchyma.[17,19] Therefore, identifying other imaging features that help distinguish between non-HCC malignancies and HCCs assigned to LR-M is worth studying.

Although rim APHE is an important targetoid feature of the LR-M category, a recent study by Choi et al[20] demonstrated that non-HCC malignancy more frequently showed thin-rim APHE on arterial phase (AP) imaging, while thick-rim APHE more frequently appeared in HCC assigned to LR-M. Some HCCs may fail to meet LR-5 criteria and may be categorized as LR-M when rim APHE is present. As a result, the subdivision of rim APHE may improve accuracy of the LI-RADS. Nonetheless, to date, the relevant studies have been limited.[17,20] Therefore, the present study aimed to identify imaging features that help distinguish between HCCs and non-HCC malignancies assigned to LR-M and to evaluate the diagnostic performance of a LI-RADS with targetoid criteria using thin-rim APHE in both ECA-MRI and HBA-MRI.

Materials and Methods
Ethics Statement
This retrospective study was approved by the Institutional Review Board of Sun Yat-sen University Cancer Center (SYSUCC), and consent for relevant procedures and the use of data for research purposes were obtained from patients before treatment. This study was conducted in accordance with the Declaration of Helsinki.

Study Subjects
Data were retrospectively collected from consecutive patients who met the following inclusion criteria in our hospital between April 2013 and March 2022: (a) Being at a high-risk of developing HCC (chronic liver disease or current/prior HCC); (b) Patients who were pathologically diagnosed by surgical resection or lesion biopsy; (c) Patients who underwent enhanced-MRI within two months prior to surgery or lesion biopsy. Finally, a total of 381 patients (322 men, 59 women) with 387 observations were included (Figure 1).

Histological Diagnosis
The tumor diagnosis was based on histopathological examination. The tumor specimens were pathologically obtained by surgical resection or lesion biopsy. Each hepatic lesion was histopathological confirmed by hepatobiliary pathologists with >10 years of experience. Tumor differentiation and histological type were assessed. The demographic and pathological characteristics of 387 observations in 381 patients are presented in Table 1.
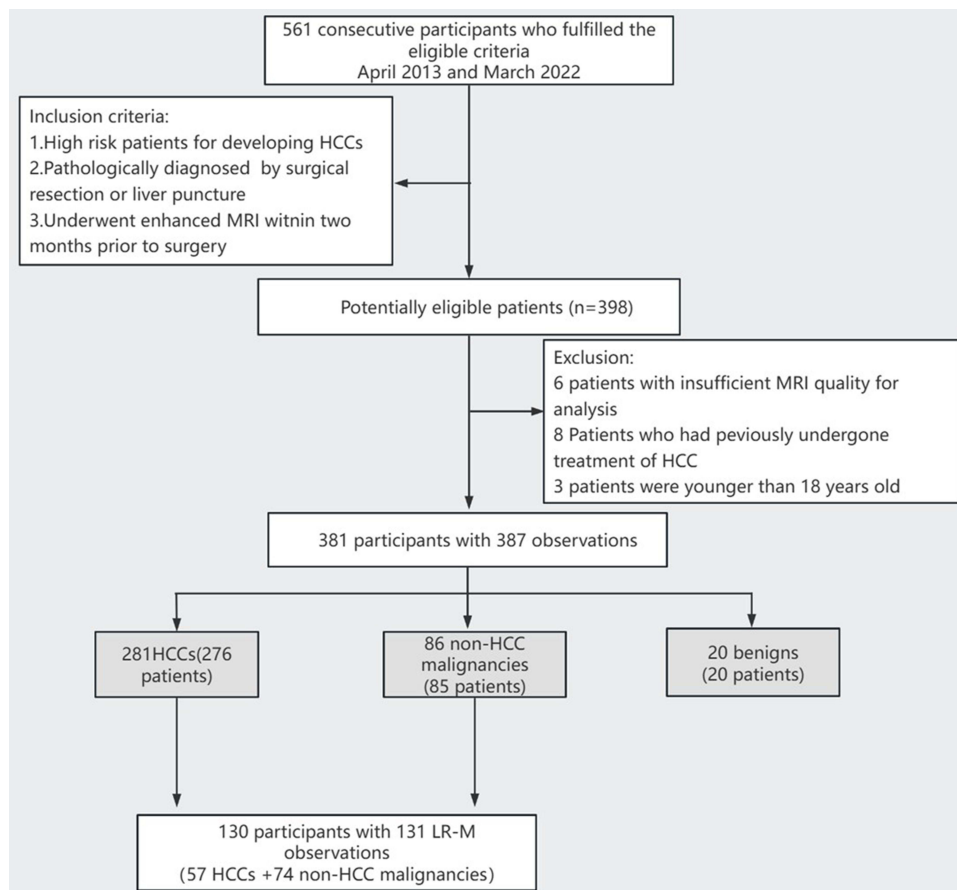
Figure 1 Flowchart of the study. HCC, hepatocellular carcinoma; LR-M, LI-RADS M.

MRI Examination

All patients underwent liver MRI examination using a 1.5T or 3T scanner (Siemens Medical Solutions, Munich, Germany; GE Health Care, New York, NY, USA; Philips Medical Systems, Amsterdam, Netherlands), and the conventional sequences included pre-contrast spin-echo T1-weighted images, fast spin-echo T2-weighted images, and gadoterate meglumine (Gd-DTPA, extracellular agent) contrast-enhanced transverse and coronal T1-weighted images. The fat suppression technique was used for fast spin-echo T2-weighted images. DWI was performed using a navigator-triggered single-shot echoplanar sequence with DW gradients (b values, 0, 800 sec/mm^2). Gadoxetic acid (Gd-EOB-DTPA, Primovist $^®$; Bayer Schering Pharma, Berlin, Germany,

Table I Demographic and Pathological Characteristics of 381 Patients with 387 Hepatic Tumors

Parameter	Value
No. of participants	n=381
Mean age (years old)	52.9±21.4
Male/Female	323/58
Cause of chronic liver disease	
Hepatitis B virus	373
Hepatitis C virus	3
Alcoholic liver disease	3
Nonalcoholic steatohepatitis	2
Liver cirrhosis	215
No. of Observations	387

(*Continued*)

Table I (Continued).

Parameter	Value
Observation size (mm)	49.2±27.2
<20	38
≥20	349
Final diagnosis	
HCC	281
Non-HCC malignancy	86
ICC	51
cHCC-CC	31
Metastasis	2
EHE	2

Note: Continuous variables are described as median with interquartile range in parenthesis. Categorical variables are described as number of participants.
Abbreviations: ICC, Intrahepatic cholangiocarcinoma; cHCC-CC: Combined hepatocellular-cholangiocarcinoma; EHE, Epithelioid hemangioendothelioma.

0.1 mL/kg) was the hepatobiliary agent used in the present study. Gadoxetic acid–enhanced T1-weighted images were obtained by a fat-suppressed three-dimensional spoiled gradient-echo sequence and volumetric interpolated breath-hold examination. Multiphase images for enhanced-MRI included AP (20–35s), PVP (60–70s), delayed phase/TP (180s), and HBP (15 and 20 min only after HBA administration) images.

Image Analysis

The MR images were evaluated independently by three abdominal radiologists (with 4, 10 and 15 years of experience in interpreting liver MRI, respectively) on a picture archiving and communication system (PACS). They were aware that the study population included patients who were at a high-risk of HCC; however, they were blinded to the pathological diagnosis of each lesion and the other reader's imaging results. For patients with multiple lesions, another reader who screened the enrollments would mark the location of the index lesion.

The reviewers assessed the location and size of the target lesion, the presence or absence of major features (APHE, non-peripheral washout, and enhancing capsule), or targetoid features (rim APHE, peripheral washout, targetoid DWI, delayed central enhancement, and targetoid TP or HBP appearance) using the LI-RADS v2018, and then assigned the LI-RADS category after applying imaging features.[1] If the observations were classified to LR-M, the three readers would simultaneously evaluate some ancillary imaging features (surface retraction, bile duct dilatation, and lobulated margin). According to results of previous studies[8,18,20] and our clinical experience, though these ancillary imaging features were not included in the LI-RADS, they might be beneficial for differential diagnosis.

In the first part, a LI-RADS category was assigned to each observation using the LI-RADS v2018 (Supplement for the LI-RADS). The conventional LR-M category was satisfied if the lesion showed targetoid appearance on MRI. Afterwards, the major features, targetoid features, and some ancillary features were compared between HCC and non-HCC malignancies. In the second step, there was a 4-week interval before the readers assigned the modified LI-RADS category according to modified targetoid features to avoid recall bias. The final results were based on consensus assessment.

Diagnostic Criteria (Development of Modified Targetoid Features for LI-RADS Category)

The rim APHE was divided into two categories, and the inclusion criteria of targetoid appearance were accordingly modified. For hepatic tumors with rim APHE, the enhancement pattern was evaluated in two sub-division: peripheral thick rim-like enhancement and thin rim-like enhancement. According to the previous research, thick-rim (30–70%) and thin-rim APHE (<30%) were based on the hyper-enhanced area of the lesion surface on an AP image.[20] The definition of thick-rim (30–70%) and thin-rim (<30%) APHE were simplified based on the thickness of the rim APHE. If the thickness of the thickest part of peripheral

hyperintensity was less than 30% of the tumor radius on the same AP image, it was defined as thin-rim APHE. On the contrary, if the thickness of the thickest part of the ring-enhancement was between 30% and 70% of the tumor radius, it was defined as thick-rim APHE (Figure 2).

In the modified LR-M criteria with modified targetoid features, the lesion was classified into LR-M as long as it showed anyone of the following appearances: thin-rim APHE, peripheral washout, delayed central enhancement, targetoid DWI or targetoid TP/HBP appearance. Accordingly, the "peripheral washout" from modified targetoid features specifically referred to the washout in which apparent washout was most pronounced in peripheral "thin-rim" of the lesion. Meanwhile, the thick-rim APHE was taken as a type of heterogeneous non-rim enhancement for the LR-5 inclusion criteria into account.

Statistical Analysis

Demographic and imaging characteristics were compared between HCC and non-HCC malignancies. Continuous variables were expressed as mean ± standard deviation, while categorical variables were expressed as number and percentage.

The Chi-square test or the Fisher's exact test were used to compare the frequency of categorical variables for differentiation of HCC and non-HCC malignancies, as well as ECA-MRI and HBA-MRI. Interobserver agreement for imaging features of LR-M observation were analyzed with k statistics and interpreted as follows: slight, 0.01–0.20; fair, 0.21–0.40; moderate, 0.41–0.60; substantial, 0.61–0.80; and excellent, 0.81–1.00.

Univariate and multivariate analysis was conducted to determine reliable predictors to differentiate between HCC and non-HCC malignancies among the LR-M lesions. $P < 0.05$ on univariate analysis was included in the multivariate logistic regression analysis. Receiver operating characteristic (ROC) curve analysis was performed to assess the diagnostic efficiency and calculate the area under the curve (AUC).

Finally, differences in diagnostic accuracy, sensitivity, specificity, positive predictive value (PPV), and negative predictive value (NPV) before and after modifying targetoid features were compared using the McNemar's test or Chi-square test. The statistical analysis was performed using SPSS 25.0 software (IBM, Armonk, NY, USA). Statistical significance was set to $P < 0.05$.
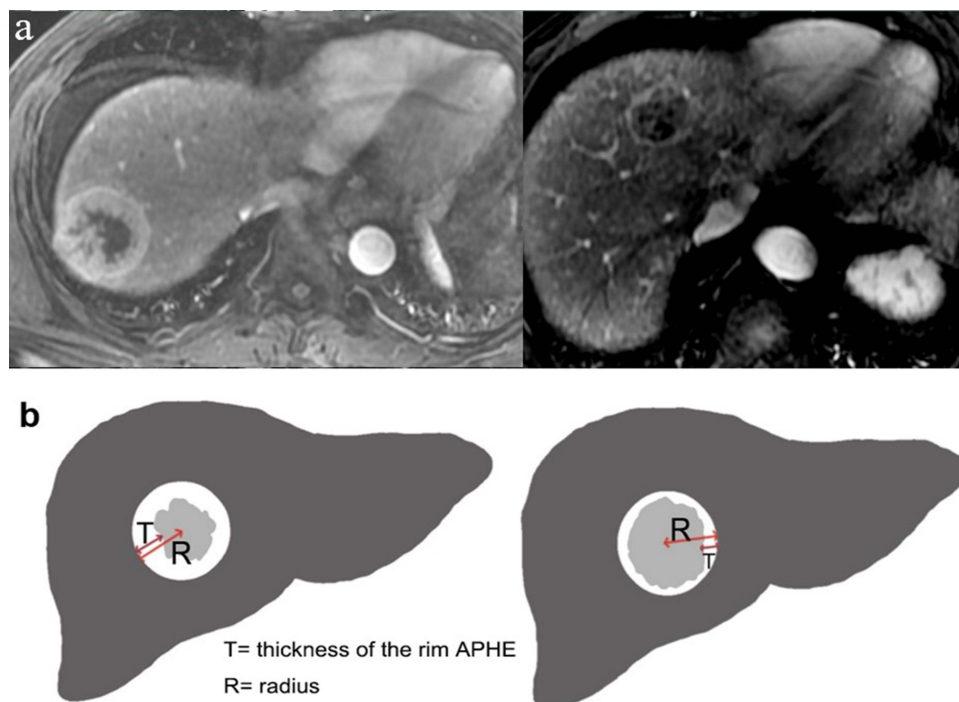
Figure 2 Rim hyperenhancement patterns on AP image and the modified measurement criterion of rim APHE. (**a**) Rim hyperenhancement patterns on AP image, thick-rim (left) and thin-rim(right). (**b**) the modified measurement criterion of rim APHE. Hepatic observations with rim APHE (spatially defined subtype of APHE in which arterial phase enhancement is most pronounced in the periphery) were divided into two categories, thick-rim (30–70%) and thin-rim APHE (< 30%). The thickness measurement of the rim APHE compared with the tumor radius is T/R=30%-70%, classified as thick-rim APHE (left). The thickness measurement of the rim APHE compared with the tumor radius is T/R<30%, classified as thin-rim APHE(right).

Results

Patients' Demographic and Pathological Characteristics

The final pathologic diagnoses of 381 participants with 387 hepatic observations were confirmed as 281 (72.6%) HCCs, 86 (22.2%) non-HCC malignancies, and 20 (5.2%) benign lesions. Histopathologic confirmation of hepatic observations was performed by segmentectomy (n = 165), lobectomy (n = 209), and liver biopsy (n=13). Of the 381 patients, 375 patients had a single nodule and 6 patients had two nodules. Hepatitis B virus infection was the most common risk factor for HCC, other causes include hepatitis C virus, alcoholic liver disease and nonalcoholic steatohepatitis.

MRI Characteristics of HCC and Non-HCC Malignancies

Of the 387 lesions, 131 (33.9%) lesions (median size, 53.5 mm) were categorized as LR-M using the LI-RADS v2018. Among the 131 LR-M observations, there were 57 (43.5%) HCCs and 74 (56.5%) non-HCC malignancies. Meanwhile, 4.2% (12/281) and 75.4% (212/281) of HCCs were classified as LR-4 and LR-5, respectively, while 2.3% (2/86) and 11.6% (10/86) of non-HCC malignancies were categorized into LR-3 and LR-5, respectively.

Table 2 shows LI-RADS category of 367 malignant lesions using conventional LI-RADS v2018. LR-5 category was predominated for HCCs (212/281, 75.4%), whereas non-HCC malignancies were mostly classified as the LR-M category (74/86, 86.0%).

The LI-RADS features of all 367 hepatic malignant observations achieved by enhanced-MRI using HBA and ECA are summarized in Table 3. There were 164 patients underwent MRI with hepatobiliary contrast agents, and 217 patients underwent MRI with extracellular contrast agents. In the Chi-square test, enhancing capsule was more commonly observed with ECA-MRI compared with HBP-MRI among HCCs (134/150 [89.3%] vs 80/131 [61.1%], $P < 0.001$). Besides, rim APHE was the most common targetoid feature found in LR-M observations, followed by delayed central enhancement, and none of them were statistically different in both types of MRI.

The histopathological subtypes of 57 HCC within the LR-M are shown in Supplementary Table 1. Among these HCCs, 35 (61.4%) were trabecular-type HCC, and 17 (29.8%) were trabecular mixed with pseudo-glandular-type HCCs. Meanwhile, HCCs with targetoid features were mostly associated with the poor differentiation (53/57, 93.0%). The majority of non-HCC malignancies included ICC and cHCC-CC.

MRI Characteristics of LR-M Observations

Univariate analysis showed that the enhancing capsule, thick-rim APHE, and peripheral washout were more frequently visualized in HCCs than in non-HCC malignancies (36/57 [63.2%] vs 8/74 [10.8%], $P < 0.001$; 39/57 [68.4%] vs 5/74 [6.8%], $P < 0.001$; 44/57 [77.2%] vs 35/74 [47.3%], $P = 0.001$) among LR-M observations (Table 4 and Figure 3). Non-HCC malignancies exhibited thin-rim APHE rather than thick-rim APHE (51/74 [68.9%] vs 11/57 [19.3%], $P < 0.001$) (Supplementary Figure 1). Besides, non-HCC malignancies more frequently had delayed central enhancement ($P<0.001$), targetoid DWI ($P=0.014$), targetoid TP/HBP ($P = 0.009$), and bile duct dilatation ($P= 0.002$) (Figure 4).

Table 2 Liver Imaging-Reporting and Data System (LI-RADS v2018) Categorization of HCC and Non-HCC Malignancies Using Contrast-Enhanced MRI

Category	HCC malignancy (n=281)	Non-HCC malignancy (n=86)	Benign lesions (n=20)
LR-3	0	2 (2.3)	13 (65.0)
LR-4	12 (4.3)	0	5 (25.0)
LR-5	212 (75.4)	10 (11.6)	2 (10.0)
LR-M	57 (20.3)	74 (86.0)	0

Note: Data in parenthesis are presented as percentage.
Abbreviations: HCC, Hepatocellular carcinoma; LR-3(LI-RADS-3), Intermediate probability of HCC; LR-4(LI-RADS-4), Probably HCC; LR-5(LI-RADS-5), Definitely HCC; LR-M(LI-RADS-M), Definitely or probably malignant.

Table 3 MRI Features of Malignant Observations According to MRI Modality (ECA-MRI Vs HBA-MRI)

LI-RADS features	HCC (n=281)			Non-HCC malignancy (n=86)		
	ECA-MRI (n=150)	HBA-MRI (n=131)	P value	ECA-MRI (n=55)	HBA-MRI (n=31)	P value
Major features						
Non-rim APHE	125 (83.3)	105 (80.2)	0.490	19 (34.5)	9 (29.0)	0.241
Non-peripheral washout	122 (81.3)	105 (80.2)	0.802	12 (21.8)	6 (19.4)	0.787
Enhancing capsule	134 (89.3)	80 (61.1)	**<0.001**	8 (14.5)	3 (9.7)	0.739
Targetoid appearance						
Rim APHE	24 (16.0)	26 (19.8)	0.400	34 (61.8)	22 (71.0)	0.393
			0.130			0.184
Thick rim	22 (91.7)	17 (65.4)		4 (11.8)	1 (4.5)	
Thin rim	2 (8.4)	9 (34.6)		29 (85.3)	21 (95.5)	
Peripheral washout	19 (12.7)	25 (19.1)	0.140	20 (36.4)	15 (48.4)	0.276
Delayed central enhancement	13 (8.7)	8 (6.1)	0.416	40 (72.7)	17 (54.8)	0.092
Targetoid DWI	6 (4.0)	7 (5.3)	0.601	17 (30.9)	15 (48.4)	0.107
Targetoid TP/HBP	NA	7 (5.3)		NA	22 (71.0)	

Note: Data in parenthesis are presented as percentage.
Abbreviations: HCC, Hepatocellular carcinoma; ECA-MRI, Extracellular contrast agent–enhanced MRI; HBA-MRI, Hepatobiliary agent–enhanced MRI; APHE, Arterial phase hyperenhancement; DWI, Diffusion-weighted imaging; TP, Transitional phase; HBP, Hepatobiliary phase; NA, Not applicable/available.

Table 4 Comparison of LI-RADS Characteristic of the Study Population Within LR-M Category

LI-RADS features	HCC (n=57)	Non-HCC malignancy (n=74)	OR (univariable)	OR (multivariable)
Major features				
Non-rim APHE	7 (12.3)	14 (18.9)	1.69 (0.65–4.78, p=0.29)	
Non-peripheral washout	5 (8.8)	8 (10.8)	0.78 (0.22–2.48, p=0.68)	
Enhancing capsule	36 (63.2)	8 (10.8)	13.93 (5.85–36.71, p<0.001)	8.38 (2.66–30.55, p=0.001)
Targetoid appearance				
Rim APHE	50 (87.7)	56 (75.7)	0.43 (0.16–1.07, p=0.08)	
Thick rim	39 (68.4)	5 (6.8)	0.03 (0.01–0.09, p<0.001)	0.07 (0.01–0.30, p=0.001)
Thin rim	11 (19.3)	51 (68.9)	0.10 (0.04–0.23, p<0.001)	0.08 (0.02–0.24, p<0.001)
Peripheral washout	44 (77.2)	35 (47.3)	0.27 (0.12–0.58, p=0.001)	0.08 (0.02–0.31, p<0.001)
Delayed central enhancement	21 (36.8)	57 (77.0)	6.11 (2.87–13.55, p<0.001)	
Targetoid DWI	13 (22.8)	32 (43.2)	2.64 (1.24–5.86, p=0.014)	7.02 (1.89–30.42, p=0.005)
Targetoid TP/HBP	7/28 (25.0)	22/29 (75.9)	0.32 (0.13–0.73, p=0.009)	
Ancillary features				
Surface retraction	9 (15.8)	27 (36.5)	0.40 (0.14–1.03, p=0.068)	
Bile duct dilatation	4 (7.0)	23 (31.1)	0.16 (0.05–0.46, p=0.002)	
Lobulated margin	17 (29.8)	33 (44.6)	1.94 (0.94–4.09, p=0.075)	

Note: Data in parenthesis are presented as percentage.
Abbreviations: HCC, Hepatocellular carcinoma; APHE, Arterial phase hyperenhancement; DWI, Diffusion-weighted imaging; TP, Transitional phase; HBP, Hepatobiliary phase.

In the multivariate analysis, thin-rim APHE ($P< 0.001$) and targetoid DWI ($P = 0.005$) were independent predictive factors of non-HCC malignancies. While enhancing capsule, thick-rim APHE and peripheral washout were independent significant variables associated with HCCs of LR-M category.
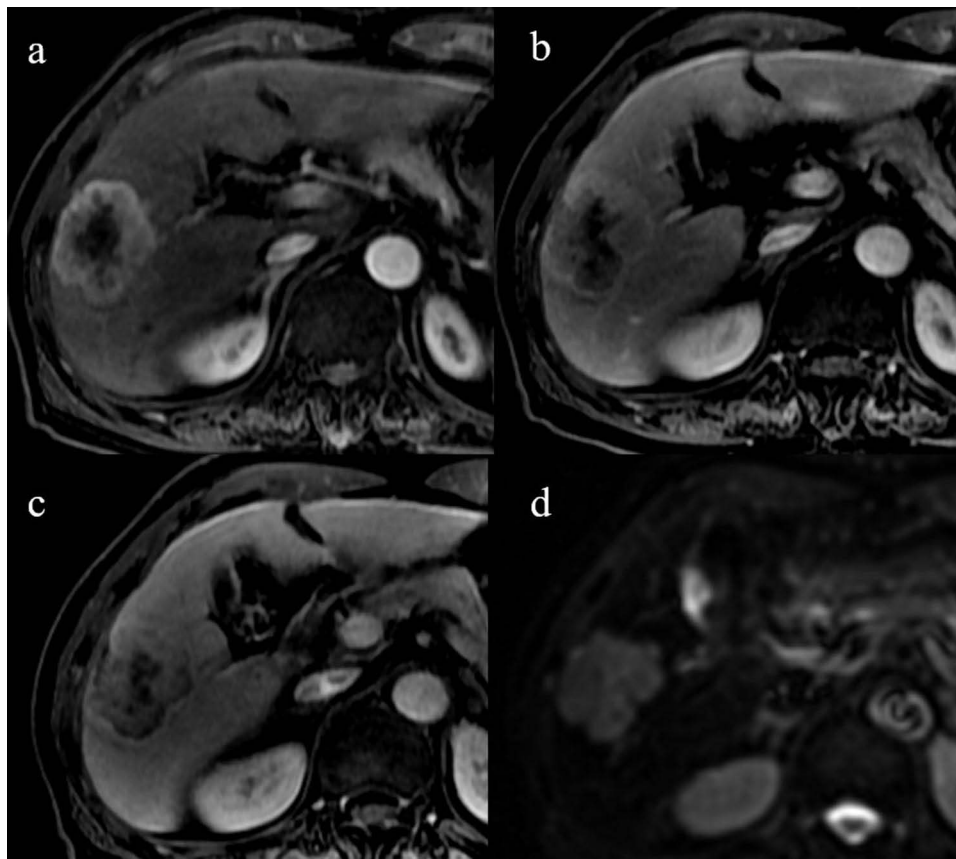
Figure 3 Hepatocellular carcinoma in a 74-year-old man with chronic hepatitis B. (**a-c**) On the axial arterial phase, portal venous phase and delayed phase images after administration of extracellular contrast agent, the segment-5 lesion showed thick-rim arterial phase hyperenhancement (APHE) followed by non-peripheral washout. (**d**) The mass showed a non-targetoid appearance on b-800 diffusion weighted image. The tumor was initially categorized as LR-M by observers. The tumor was re-categorized as modified LR-5 according to modified LI-RADS.

A ROC curve was plotted to evaluate the diagnostic performance of the three significant targetoid features (thin-rim APHE, targetoid DWI, and peripheral washout). As shown in Figure 5, thin-rim APHE showed a noticeable diagnostic performance in distinguishing non-HCC malignancies from HCCs (AUC (thin-rim APHE) = 0.75, 95% confidence interval (CI): 0.66–0.83; AUC (peripheral washout) = 0.65, 95% CI: 0.56–0.75; and AUC (targetoid DWI) =0.53, 95% CI: 0.43–0.63).

Diagnostic Performance of the Modified LI-RADS

The modified LI-RADS emphasizing thin-rim APHE instead of rim APHE was established. Sensitivity, specificity, accuracy, PPV, and NPV of the conventional and modified LI-RADS are presented in Table 5. Compared with the conventional LI-RADS v2018, the modified LR-M attained significantly higher values of specificity and accuracy (81.1% vs 89.4%, $P = 0.004$; and 82.2% vs 87.9%, $P=0.027$, respectively), while maintaining a high sensitivity (86.0% vs 82.2%; $P=0.529$) for non-HCC malignancies. Meanwhile, the modified LR-5 achieved greater values of sensitivity and accuracy (88.6% vs 79.7%, $P= 0.004$; and 85.8% vs 80.1%, $P= 0.036$, respectively) for diagnosing HCC, without compromising specificity (81.1% vs 78.3%; $P=0.608$) when compared with LI-RADS v2018. The sensitivity of the modified LR-M and the specificity of the modified LR-5 were slightly reduced due to the fact that three non-HCC malignancies had no other targetoid features, except for the thick-rim APHE, and they were misclassified as the modified LR-5.

Interobserver agreement (IOA)

The IOA values of MRI features and LI-RADS categories for the diagnosis of hepatic lesions are listed in Supplementary Table 2. The IOA was substantial to excellent for all features (κ =0.614–0.840).
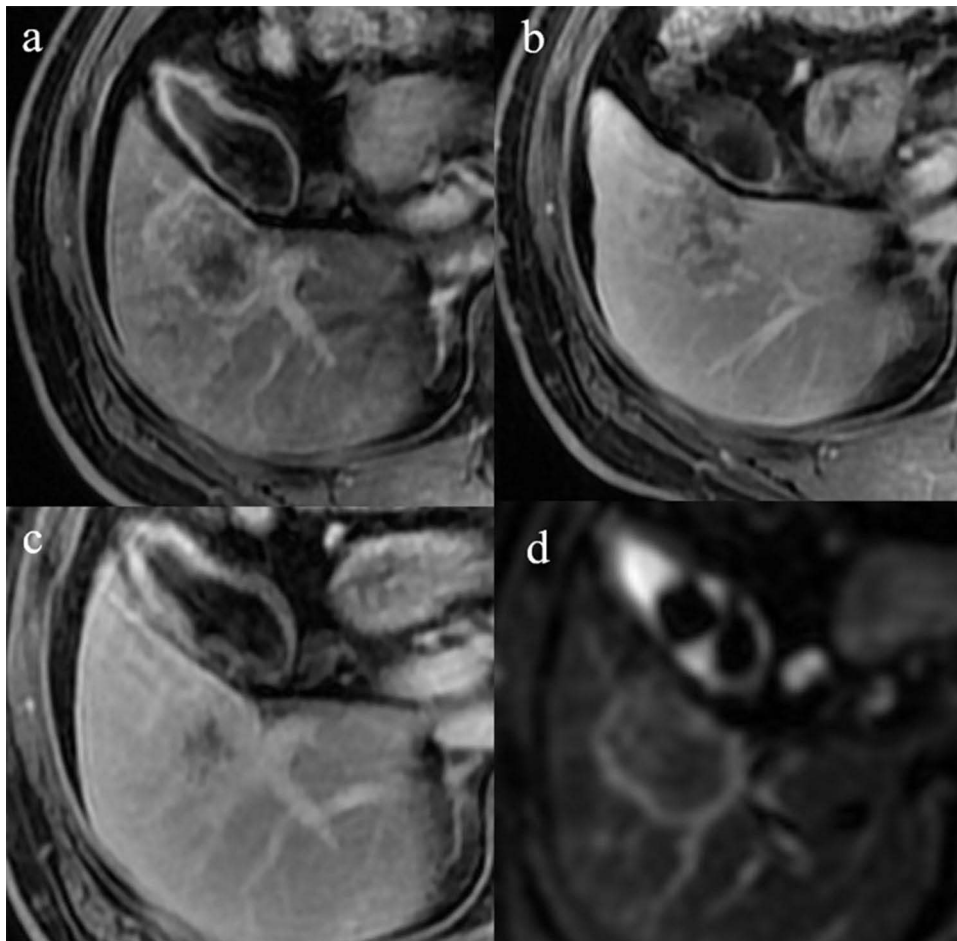
Figure 4 Intrahepatic cholangiocarcinoma in two patients, a 48-year-old man with chronic hepatitis B. On the axial arterial phase image (**a**), the liver mass on segment 5 showed thin-rim arterial phase hyperenhancement (APHE). On portal venous phase and delayed phase images (**b** and **c**) after administration of extracellular contrast agent, the tumor showed delayed central enhancement. On b-800 DWI image (**d**), the mass showed a targetoid appearance. The tumor was initially categorized as LR-M by observers. The tumor was re-categorized as modified LR-M according to modified LI-RADS.
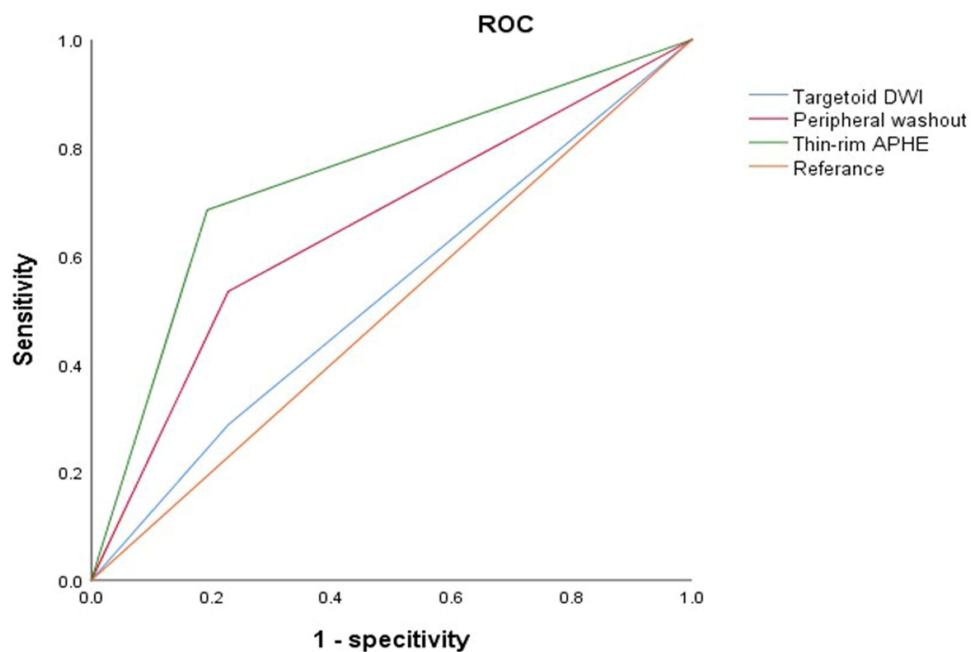
Figure 5 Performance of thin-rim APHE, targetoid DWI and peripheral washout to distinguish non-HCC malignancy from HCC in targetoid lesions.

Table 5 Diagnostic Performance of LI-RADS Categories for the Diagnosis of Hepatic Malignancies Using Enhanced MRI

	TP	FN	FP	TN	Sensitivity (95% CI)	Specificity (95% CI)	Accuracy (95% CI)	PPV (95% CI)	NPV (95% CI)
LR-M	74	12	57	244	86.0 (78.6–93.5)	81.1 (76.6–85.5)	82.2 (78.3–86.0)	56.5 (47.9–65.1)	95.3 (92.7–97.9)
mLR-M	71	15	32	269	82.2 (74.4–90.7)	89.4 (85.9–92.9)	87.9 (84.6–91.1)	68.9 (59.8–78.0)	94.7 (92.1–97.3)
P value					0.529	0.004	0.027	NA	NA
LR-5	224	57	20	86	79.7 (75.0–84.4)	81.1 (73.6–88.7)	80.1 (76.1–84.1)	91.8 (88.3–95.3)	60.1 (52.0–68.3)
mLR-5	249	32	23	83	88.6 (84.9–92.3)	78.3 (70.3–86.3)	85.8 (82.3–89.3)	91.5 (88.2–94.9)	72.2 (63.9–80.5)
P value					0.004	0.608	0.036	NA	NA

Note: Data are described as percentage with 95% confidence interval in parenthesis.
Abbreviations: TP, True positive; FN, False negative; FP, False-positive; TN, True negative; CI, Confidence interval; PPV, Positive predictive value; NPV, Negative predictive value; LR-M, LI-RADS M; mLR-M, Modified LI-RADS M; mLR-5, Modified LI-RADS 5; NA, Not applicable.

Discussion

Although previous studies provided data for differentiating non-HCC malignancy from atypical HCC categorized as LR-M,[6,17,21,22] no study has yet concentrated on revising targetoid features for the LR-M category. The present research revealed that some MRI features (as shown in Table 4) can be used to distinguish between HCC and non-HCC malignancy in the LR-M category. Among three significant targetoid appearances (thin-rim APHE, targetoid DWI and peripheral washout), thin-rim APHE exhibited a greater diagnostic ability for non-HCC malignancies compared with the others. Therefore, thin-rim APHE might serve as a modified targetoid feature to improve the diagnostic performance of the LI-RADS for malignant hepatic tumors. It was indicated that LR-M with the modified targetoid features outperformed the conventional LR-M in terms of both specificity and accuracy, and the modified LR-5 correspondingly showed greater sensitivity and accuracy compared with the LR-5.

Enhancing capsule, which may serve as a major feature, is essential for the diagnosis of HCC.[9,13] Accordingly, in our study, the enhancing capsule was more frequently detected in HCCs than in non-HCC malignancies. Although capsule appearance is a characteristic feature favoring HCC, the display of capsule is also limited by the use of contrast medium (gadoxetic acid) for MRI,[17,19] because the early uptake of contrast media by hepatocytes could obscure capsule appearance. In our study, enhancing capsule was more highly revealed by ECA-MRI than HBA-MRI, which is in line with Min et al's findings.[17] As a result, the application of enhancing capsule to identify HCC with targetoid features from LR-M may be more challenging in HBA-MRI than in ECA-MRI.

In contrast to enhancing capsule, the rim APHE was reported as the dominant targetoid feature for the identification of non-HCC malignancy.[9] A meta-analysis demonstrated that among all targetoid features, the rim APHE was more frequently found in both HCC and non-HCC malignancy assigned to LR-M.[8] Similarly, the rim-APHE was identified in approximately 80% (106/131) of our LR-M cases and it appeared almost equally on both HBA-MRI and ECA-MRI. On the other hand, a recent study revealed that some tumors with thick-rim APHE, a more common imaging feature of HCC rather than non-HCC malignancy, should not be classified to LR-M.[17] It suggested that further subdividing rim APHE into thick-rim and thin-rim APHE may help distinguish between non-HCC malignancy and HCC in LR-M. The present research revealed that thick-rim APHE and peripheral washout were more frequently detected in atypical HCCs, and thin-rim APHE was more likely found in non-HCC malignancies in MRI. The appearance of the thick-rim APHE could be attributed to the central necrosis and quite a few viable tumor cells in the periphery of the large atypical HCCs, while the thin-rim APHE in ICCs may result from fewer viable tumor cells in peripheral region of ICCs with a large amount of fibrous tissue in the center, as well as the congestive hepatopathy with dilated sinusoids around the tumor.[23,24] Moreover, the reason why peripheral washout appeared mostly in atypical HCCs from present study is probably because these HCCs exhibited thick-rim APHE followed by atypical "peripheral washout". It also illustrated the importance of accurate definition of the thick-rim APHE and thin-rim APHE as it might provide a more precise definition of "peripheral washout", which could likewise help improve the diagnostic performance of LI-RADS.

In addition to thin-rim APHE, targetoid DWI also performed well in distinguishing non-HCC malignancy from HCC assigned to LR-M. Targetoid DWI was reported to be indicative of non-HCC malignancies rather than HCCs.[21] Similarly,

the present study demonstrated the same results. Although previous studies[18,20] pointed toward the value of some ancillary features in differentiating non-HCC malignancies from HCCs, these studies were restricted to small cohort studies of LR-M patients and then such ancillary features appeared in a relatively small number of cases; therefore, further large sample size study is needed to validate this finding.

To date, there is still a big gap to fill in the modification of LI-RADS criteria.[23,24] The LR-M category was designed to preserve the high specificity of LR-5 category; thus, its specificity and accuracy for non-HCC malignancies were relatively low. In our study, almost 70% (51/74) of non-HCC malignancies of LR-M cases showed thin-rim APHE. Besides, when evaluated by ROC curve, thin-rim APHE stood out more prominently in distinguishing non-HCC malignancies from HCC compared with other targetoid features. The results suggested that thin-rim APHE might serve as a significant imaging feature to categorize an observation as the LR-M category. Therefore, the modified LR-M category in our study placed great emphasis on the thin-rim APHE and it demonstrated superior specificity and accuracy for diagnosing non-HCC malignancies versus the conventional LR-M criteria. Meanwhile, there was no significant difference in sensitivity between conventional and modified LR-M. Theoretically, there is a risk that the sensitivity of LR-M may slightly decrease while applying the modified criterion. In our study, three non-HCC malignancies, which included two ICCs and one cHCC-CC, were misclassified as LR-5 because they had no other targetoid features except for the thick-rim APHE. However, the modified LR-5 category, which took into account the thick-rim APHE, significantly improved sensitivity and accuracy in our cases; in a word, the subdivision of rim APHE can lead to an increase in diagnostic performance of LI-RADS as a whole.

The present study has several potential limitations. First, selection bias was inevitable because it was a retrospective study. Second, it was a single-center observational study and the disease distribution in the center likely differs from that encountered in a general community setting. This may account for the lower specificity of LR-5 for HCC in this study than expected. Third, pathological findings in some cases were confirmed by biopsy rather than the entire surgical specimen, and it created the possibility of biopsy sampling errors. Forth, some patients underwent ECA-MRI examination and the others underwent HBA-MRI examination, which might introduce bias in the results.

In conclusion, the accurate definition of the thick-rim APHE and thin-rim APHE may be valuable, and thin-rim APHE may be the most important imaging feature for differentiating non-HCC malignancies from HCCs within LR-M in MRI. With emphasizing the thin-rim APHE in targetoid features, a modified LI-RADS category was established, which showed a greater specificity for non-HCC malignancies and a superior sensitivity for HCCs versus conventional criteria, without compromising sensitivity of the LR-M category and specificity of the LR-5 category. Larger and prospective studies may help to further validate these findings in the future.

Abbreviations

LI-RADS v2018, Liver Imaging Reporting and Data System version 2018; LR-M, LI-RADS M; LR-5, LI-RADS 5; APHE, Arterial phase hyperenhancement; DWI, Diffusion-weighted imaging; ECA, Extracellular agent; TP, Transitional phase; HBP, Hepatobiliary phase; AP, arterial phase; PVP, Portal venous phase; HBA, Hepatobiliary agent; HCC, Hepatocellular carcinoma; ICC, Intrahepatic cholangiocarcinoma; cHCC-CC, Combined hepatocellular-cholangiocarcinoma; mLR-M, Modified LI-RADS M; mLR-5, Modified LI-RADS 5; MRI, Magnetic resonance imaging; NPV, Negative predictive value; PPV, Positive predictive value; IOA, Interobserver agreement.

Disclosure

The authors report no conflicts of interest in this work.

References

1. American College of Radiology. Liver Imaging reporting and data system version 2018. Available from: http://www.acr.org/QualitySafety/Resources/LIRADS. Accessed April 04, 2024.
2. Huang Z, Zhou PP, Li SS, Li K. CEUS LI-RADS for diagnosis of hepatocellular carcinoma in individuals without LI-RADS-defined hepatocellular carcinoma risk factors. *Cancer Imaging*. 2023;23(1):24. doi:10.1186/s40644-023-00541-2
3. Chernyak V, Fowler KJ, Kamaya A, et al. Liver imaging reporting and data system (LI-RADS) version 2018: imaging of hepatocellular carcinoma in at-risk patients. *Radiology*. 2018;289(3):816–830. doi:10.1148/radiol.2018181494

4. Park JG, Jung GS, Yun JH, et al. Percutaneous transluminal forceps biopsy in patients suspected of having malignant biliary obstruction: factors influencing the outcomes of 271 patients. *Eur Radiol*. 2017;27(10):4291–4297. doi:10.1007/s00330-017-4796-x

5. An C, Park S, Chung YE, et al. Curative resection of single primary hepatic malignancy: liver imaging reporting and data system category LR-M portends a worse prognosis. *AJR Am J Roentgenol*. 2017;209(3):576–583. doi:10.2214/ajr.16.17478

6. Jang JK, Choi SH, Byun JH, et al. New strategy for liver imaging reporting and data system category M to improve diagnostic performance of MRI for hepatocellular carcinoma ≤ 3.0 cm. *Abdom Radiol*. 2022;47(7):2289–2298. doi:10.1007/s00261-022-03538-w

7. Li Y, Ni X, Liu X, et al. Prognosis of primary liver cancer based on LI-RADS classification with extracellular agent-enhanced MRI. *J Hepatocell Carcinoma*. 2023;10:399–411. doi:10.2147/jhc.S394840

8. Kim DH, Choi SH, Park SH, et al. Liver imaging reporting and data system category M: a systematic review and meta-analysis. *Liver Int*. 2020;40(6):1477–1487. doi:10.1111/liv.14420

9. Kim YY, Kim MJ, Kim EH, Roh YH, An C. Hepatocellular carcinoma versus other hepatic malignancy in cirrhosis: performance of LI-RADS version 2018. *Radiology*. 2019;291(1):72–80. doi:10.1148/radiol.2019181995

10. Kierans AS, Makkar J, Guniganti P, et al. Validation of liver imaging reporting and data system 2017 (LI-RADS) criteria for imaging diagnosis of hepatocellular carcinoma. *J Magn Reson Imaging*. 2019;49(7):e205–e215. doi:10.1002/jmri.26329

11. Lee SM, Lee JM, Ahn SJ, Kang HJ, Yang HK, Yoon JH. LI-RADS version 2017 versus version 2018: diagnosis of hepatocellular carcinoma on gadoxetate disodium-enhanced MRI. *Radiology*. 2019;292(3):655–663. doi:10.1148/radiol.2019182867

12. Tang A, Bashir MR, Corwin MT, et al. Evidence Supporting LI-RADS Major Features for CT- and MR imaging–based diagnosis of hepatocellular carcinoma: a systematic review. *Radiology*. 2018;286(1):29–48. doi:10.1148/radiol.2017170554

13. Park HJ, Kim YK, Cha DI, et al. Targetoid hepatic observations on gadoxetic acid-enhanced MRI using LI-RADS version 2018: emphasis on hepatocellular carcinomas assigned to the LR-M category. *Clin Radiol*. 2020;75(6):478.e13–478.e23. doi:10.1016/j.crad.2020.01.002

14. van der Pol CB, Lim CS, Sirlin CB, et al. Accuracy of the liver imaging reporting and data system in computed tomography and magnetic resonance image analysis of hepatocellular carcinoma or overall malignancy-a systematic review. *Gastroenterology*. 2019;156(4):976–986. doi:10.1053/j.gastro.2018.11.020

15. Min JH, Lee MW, Park HS, et al. LI-RADS version 2018 targetoid appearances on gadoxetic acid-enhanced MRI: interobserver agreement and diagnostic performance for the differentiation of HCC and Non-HCC malignancy. *AJR Am J Roentgenol*. 2022;219(3):421–432. doi:10.2214/ajr.22.27380

16. Kim JH, Joo I, Lee JM. Atypical appearance of hepatocellular carcinoma and its mimickers: how to solve challenging cases using gadoxetic acid-enhanced liver magnetic resonance imaging. *Korean J Radiol*. 2019;20(7):1019–1041. doi:10.3348/kjr.2018.0636

17. Min JH, Kim JM, Kim YK, et al. A modified LI-RADS: targetoid tumors with enhancing capsule can be diagnosed as HCC instead of LR-M lesions. *Eur Radiol*. 2022;32(2):912–922. doi:10.1007/s00330-021-08124-0

18. Zheng W, Huang H, She D, et al. Added-value of ancillary imaging features for differentiating hepatocellular carcinoma from intrahepatic mass-forming cholangiocarcinoma on Gd-BOPTA-enhanced MRI in LI-RADS M. *Abdom Radiol*. 2022;47(3):957–968. doi:10.1007/s00261-021-03380-6

19. Santillan C, Fowler K, Kono Y, Chernyak V. LI-RADS major features: CT, MRI with extracellular agents, and MRI with hepatobiliary agents. *Abdom Radiol*. 2018;43(1):75–81. doi:10.1007/s00261-017-1291-4

20. Choi SY, Kim YK, Min JH, et al. Added value of ancillary imaging features for differentiating scirrhous hepatocellular carcinoma from intrahepatic cholangiocarcinoma on gadoxetic acid-enhanced MR imaging. *Eur Radiol*. 2018;28(6):2549–2560. doi:10.1007/s00330-017-5196-y

21. Cha DI, Choi GS, Kim YK, et al. Extracellular contrast-enhanced MRI with diffusion-weighted imaging for HCC diagnosis: prospective comparison with gadoxetic acid using LI-RADS. *Eur Radiol*. 2020;30(7):3723–3734. doi:10.1007/s00330-020-06753-5

22. Li F, Li Q, Liu Y, et al. Distinguishing intrahepatic cholangiocarcinoma from hepatocellular carcinoma in patients with and without risks: the evaluation of the LR-M criteria of contrast-enhanced ultrasound liver imaging reporting and data system version 2017. *Eur Radiol*. 2020;30(1):461–470. doi:10.1007/s00330-019-06317-2

23. Kang Y, Lee JM, Kim SH, Han JK, Choi BI. Intrahepatic mass-forming cholangiocarcinoma: enhancement patterns on gadoxetic acid-enhanced MR images. *Radiology*. 2012;264(3):751–760. doi:10.1148/radiol.12112308

24. Murakami T, Nakamura H, Tsuda K, et al. Contrast-enhanced MR imaging of intrahepatic cholangiocarcinoma: pathologic correlation study. *J Magn Reson Imaging*. 1995;5(2):165–170. doi:10.1002/jmri.1880050210